

Environmentally friendly preparation of robust superhydrophobic surfaces on stainless steel mesh

K. K. Hou^{a,*}, Y. W. Meng^b, X. H. Chen^a, M. M. Xu^a, D. Wang^a

^aCollege of Chemical Engineering and Materials, Xuchang University, Xuchang, 461000, China

^bCollege of Information Engineering, Xuchang University, Xuchang, 461000, China

In this work, a robust surface with superhydrophobic properties was prepared on stainless steel mesh by electrodeposition combined with low surface energy modification method. The wettability, phase composition, morphology and properties of the coating were characterized and tested using dynamic contact angle measuring instrument, X-ray diffraction (XRD), scanning electron microscopy (SEM) and other techniques. The experimental results show that the synergistic effect of dense petal-like micro-nano rough structures and stearic acid modification on the surface of stainless steel mesh endow the mesh with good superhydrophobicity, so the contact angle is even up to 170.3°. In addition, it had good performances of self-cleaning, anti-friction and oil-water separation. Its water contact angle was above 150.0° even after 230 cm friction distance. Its oil-water separation efficiency did not significantly decrease after 10 times of repeated use.

(Received December 10, 2021; Accepted March 17, 2022)

Keywords: Superhydrophobic, Electrodeposition, Zinc coating, Environmentally, Robust

1. Introduction

With the development of industrialization, the pollution of oil and organic solvents on water resources has seriously affected people's production and life[1-3]. It not only destroys water resources, but also wastes a lot of non-renewable resources. How to effectively collect and remove oil and organic pollutants has become a world-class challenge[4]. Oil-water separation is an important process to treat oily wastewater. However, the traditional methods of removing oil from water are not only difficult to recycle, low separation efficiency, poor adsorption performance, but also obviously damage the natural environment and high cost limitations[5-7]. In order to realize the maximization of resources, people are inspired by the special infiltration phenomenon of nature. Recently, the use of special infiltration of materials on the different effects of water and oil to achieve oil-water separation has attracted widespread attention [8-10].

Superhydrophobic omentum or three-dimensional porous material is a new kind of oil-water separation tool, which has water-blocking and oil-transferring properties. It can not only selectively separate oil and water efficiently, but also can be reused many times. It has great application prospect in the field of oil-water separation [11-15]. At present, the preparation methods of superhydrophobic oil-water separation material are spraying method, etching method, hydrothermal method, electrodeposition method and so on [16-19]. In 2004, Jiang et al. firstly

* Corresponding author: houkeke0370@163.com

reported a method of PTFE spraying stainless steel mesh to prepare superhydrophobic mesh, and achieved oil-water mixture separation [20]. Wu et al. immersed the metal-based mesh in the mixed solution containing ferric chloride, hydrochloric acid, perfluorooctyl triethoxysilane (PTES) and ethanol to prepare bionic multifunctional superhydrophobic stainless steel mesh and copper mesh, and the mesh has good anti-icing, corrosion resistance and oil-water separation functions [21]. Tie et al. dipped, brushed, or sprayed a mixture solution concluding hydrophilic nanoparticles (TiO_2 , SiO_2 , and Al_2O_3) and fluorocarbon surfactants onto various substrates (such as fabric, sponge, cotton, stainless steel mesh and so on), and obtained superhydrophobic and underwater superoleophobic coatings with contact angles above 150° and sliding angles below 10° , in which the resistance to liquid impact, sandpaper abrasion, and acid/base treatment is excellent [22]. The preparation of the above-mentioned superhydrophobic materials may involve harsh experimental conditions, multistep procedures, or use of environmentally harmful substances. Thus it is not suitable to expand the scale in practical application.

As a commonly used surface treatment technology, electrodeposition not only has the advantages of simple equipment and operation, fast deposition rate, low cost, easy control, etc., but also can realize diversified regulation of coating surface morphology and composition by adjusting the electrodeposition parameters [23-26], showing great potential in the regulation and construction of micro-nano structure on the surface of superhydrophobic coating. Wang et al. prepared multifunctional zinc (Zn)/polydopamine (pDop)/n-dodecyl mercaptan (NDM) composite coatings with excellent superhydrophobic properties on different metal substrates (steel, aluminum and copper) by electrodeposition [27]. Chen et al. constructed superhydrophobic Nano Cu/ Al_2O_3 Ni-Cr composited coating with low adhesive force on Q345 carbon steel by electrochemical deposition [28]. By using controlled electrodeposition and chemical modification, Wu et al. obtained the superhydrophobic/ superlipophilic three dimensional porous foam copper, which could effectively separate many kinds of oil-water emulsions [29]. In the above process of obtaining superhydrophobic surface, most of the plating solutions used for electrodeposition are difficult to treat the waste liquid because of their complex components and various additives.

In this study, an electrodeposition solution with the simplest composition was used to prepare a uniform superhydrophobic composite coating on the surface of the stainless steel mesh through electrodeposition and modification with fluorine-free low surface energy material. Compared with other similar superhydrophobic surface preparation methods, this method has the advantages of simplicity, practicality, environmental protection and adjustable performance. At the same time, we further proved that our prepared superhydrophobic stainless steel mesh has excellent self-cleaning, wear-resistant and oil-water separation properties.

2. Experimental section

2.1. Fabrication of the superhydrophobic surface

2.1.1. Pretreatment of stainless steel mesh

Stainless steel mesh with a pore size of $34\ \mu\text{m}$, which had been cleaned in acetone and absolute ethanol for 10 minutes and rinsed with deionized water, was used as substrate. The as-cleaned mesh was immersed in an aqueous H_2SO_4 solution (10%) for 20 minutes to remove the

oxidation layer and residual oil [30]. After that, taken out the mesh, rinsed it with deionized water, and then dried it at 80 °C for standby.

2.1.2. Electrodeposition process

The electrodeposition solution was prepared by dissolving 50.00 g KCl, 17.50 g ZnCl₂ and 7.00 g H₃BO₃ in 250 ml deionized water, and then adjusted their pH value to about 4.8 with hydrochloric acid solution. The pretreated stainless steel mesh was connected with the negative pole of the stabilized DC power supply as the electrodeposition cathode, and the zinc electrode was connected with the positive pole of the power supply as the anode. In order to study the influence of electrodeposition conditions on the wettability, different surfaces were prepared with different electrodeposition periods (3, 5, 8 and 10 minutes) and different current densities (4.3, 4.6, 4.8, 5.2, 5.4, 5.7 and 6.0 A·dm⁻²). The whole electrodeposition processes were carried out at the temperature of 25 °C.

2.1.3. Surface modification

After electrodeposition, the mesh was rinsed with deionized water and dried at 80 °C for 1 h. Subsequently, the mesh was immersed into an ethanol solution of 0.01 M stearic acid for 3 h and then dried at 80 °C for 30 minutes. Finally, the superhydrophobic stainless steel mesh was obtained.

2.2. Characterization techniques

The crystal phases of the samples were investigated using a Bruker D8 ADVANCE powder X-ray diffractometer with Cu K α radiation. A FE-SEM (Nova NanoSEM 450) was used to examine the morphology of stainless steel mesh surface. The hydrophobicity of the stainless steel meshes was evaluated by measuring their contact angles with deionized water, where the static contact angles (CA) of as-prepared samples were measured on a goniometer (C601 solid/liquid interface analyzer, Shanghai Solon Information Technology Co., Ltd.). The static contact angles were averaged values by measuring at least five different points on each sample surface with a deionized water drop of about 3 μ L.

2.3. Mechanical durability test

Abrasion test was used to evaluate the mechanical durability of the as-prepared superhydrophobic surfaces. Firstly, cut the as-prepared samples into a square of 1.0 cm \times 1.0 cm and fixed it on the resin sheet with double-sided adhesive tape. And then cut the sandpaper (grit no. 600) into a strip of 4.0 cm \times 23.0 cm and put it on the stainless steel mesh. Finally, put 200 g weight on the corresponding position of the sandpaper. The abrasion resistance of the as-prepared samples were tested by pulling the sandpaper to move a certain distance at the speed of 2.0 cm·s⁻¹. The contact angles of the sample surfaces were then measured after pulling a certain distance.

2.4. Oil-water separation

Simple and homemade oil-water separation device was used to evaluate the oil-water separation properties of the as-prepared samples, a mixture of deionized water and oil dyed with methyl orange (edible oil, diesel oil, liquid paraffin, cyclohexane and petroleum ether, were used respectively) in a 1:2 v/v ratio was poured into the upper device, the oil freely permeated through the superhydrophobic strainer, and then fell into the beaker beneath it. Meanwhile, more and more water was accumulated on the superhydrophobic surface, and then decanted into another beaker. Because the separated oil contained little water and the error was smaller, it was reasonable to

calculate the separation efficiency with the oil quality. Therefore, the separation efficiency (η , %) was calculated by the ratio between the mass of the separated oil (m_1) and the initial oil in the mixtures (m_0). The separation efficiency was calculated by:

$$\eta(\%) = m_1 / m_0 \times 100\% \quad (1)$$

3. Results and discussion

3.1. Crystal phases and morphologies of the superhydrophobic surfaces

XRD analysis was performed to investigate the crystal phases of the as-received superhydrophobic mesh surfaces. From the full survey spectrum (Fig.1b), the diffraction peaks at 2θ values of 36.21° , 38.95° , 43.17° , 54.33° , 70.08° , 77.16° , 82.16° and 86.55° just correspond to (002), (100), (101), (102), (103), (004), (112) and (201) planes of the crystalline zinc, which are in agreement with the values in the standard card (JCPDS, 87- 0713). The other stronger diffraction peaks at the angles of 43.98° , 51.21° , and 74.87° , are the XRD peaks of stainless steel mesh substrate (Fig.1a, Marked with \blacklozenge). In addition, the sharp peaks of Fig.1b indicate that the zinc coating on the stainless steel mesh has a high degree of crystallization.

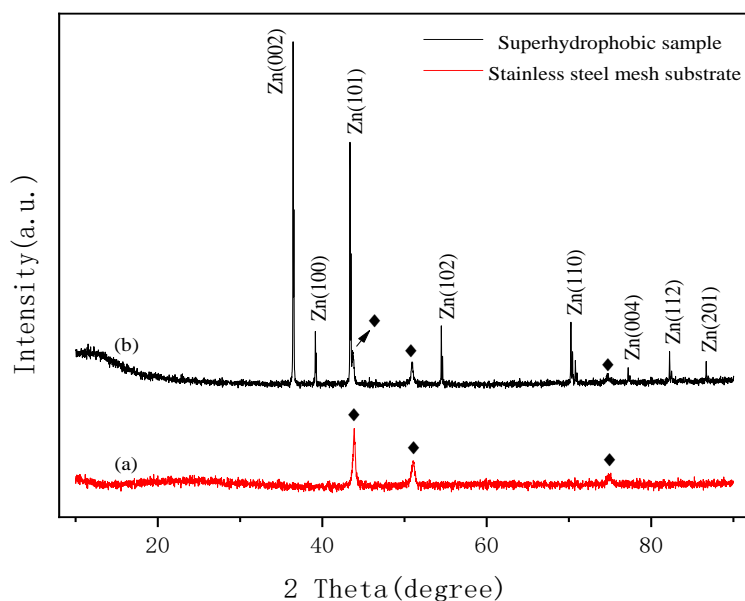


Fig. 1. XRD patterns for the blank mesh (a) and the as-prepared superhydrophobic sample (b).

The SEM micrographs of blank base and as-prepared superhydrophobic samples are shown in Fig.2. It can be seen that the surface of blank base is smooth, and there is no other rough structure except the scratch caused by sandpaper grinding (Fig.2a-b), while a dense coating was deposited on the surface of the as-prepared superhydrophobic samples (Fig.2c-d). In particular, under higher magnification, it was apparent that the surface was densely covered by petal-like structure, and the porous sponge structure was found between petals (Fig.2d). The above structures

on the surface of the samples greatly increased the surface roughness, which laid a good morphological foundation for the preparation of superhydrophobic surface.

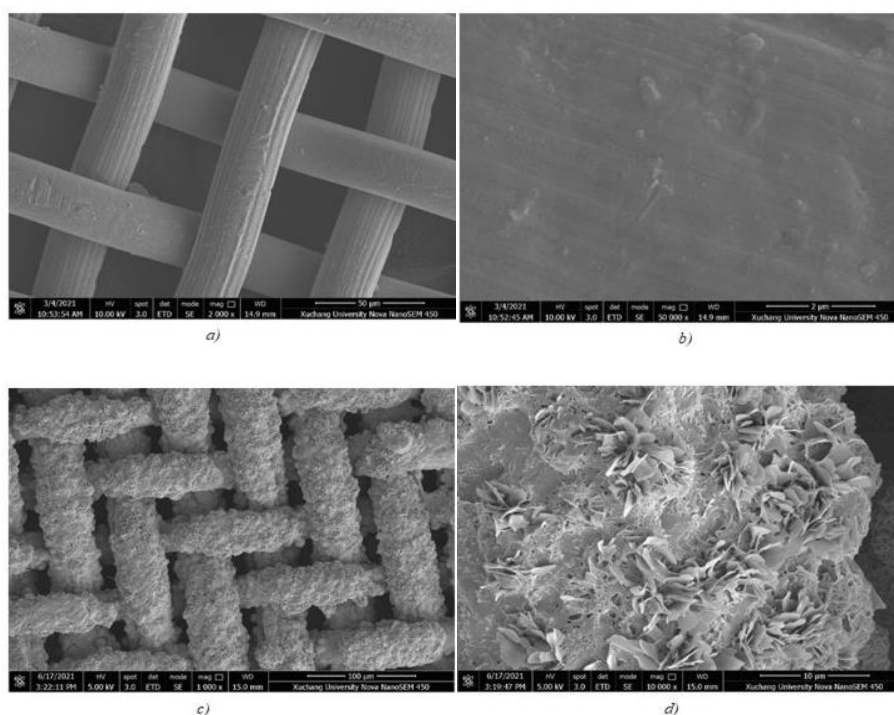


Fig. 2. SEM images of blank mesh and prepared sample with different magnification: (a) blank(2000 times); (b) blank(50000 times); (c) sample(1000 times); (d) sample(10000 times).

3.2. Mechanical durability of the superhydrophobic surfaces

The schematic illustration of the sandpaper abrasion test is shown in Fig.3a. The contact angles of the sample were measured after pulling a certain distance, and the data are shown in Fig.3b. It can be seen that the contact angles of the as-prepared sample decreased after friction of 230 cm distance, but the contact angle was still above 150.0° and still had superhydrophobic property. Therefore, the test results show that the as-prepared samples have wear-resistant and robust superhydrophobic surfaces.

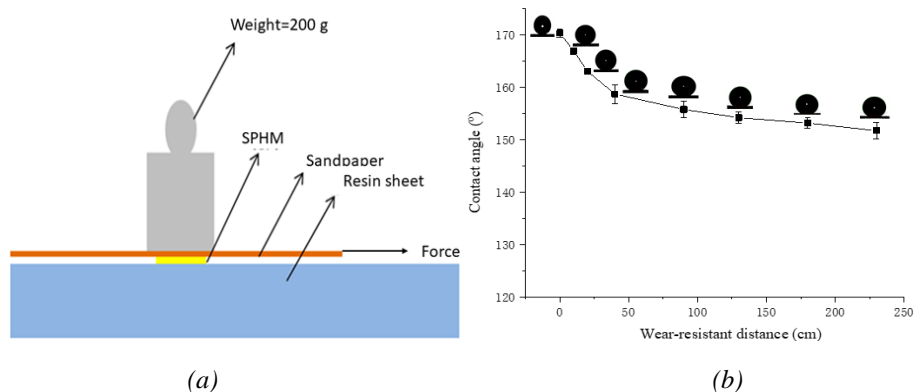


Fig. 3. (a) Schematic illustration of the sandpaper abrasion tests for the as-prepared sample at 200 g loading on the 600 mesh sandpaper. (b) Chang in WCA on the superhydrophobic stainless steel

mesh surface during the abrasion of 230 cm.

3.3. Self-cleaning property

To investigate the self-cleaning performance, chalk powder was used to simulate the dust, as shown in Fig.4a-c, the as-prepared sample was placed on a glass dish obliquely, the dust was sprinkled on the surface of the sample (Fig.4a). When the water droplets were dripped onto the sample surface, the chalk powder would be collected rapidly and thoroughly, and there was no dust residue on the sample surface (Fig.4c). This result indicates that the as-prepared superhydrophobic surfaces have excellent self-cleaning performance.

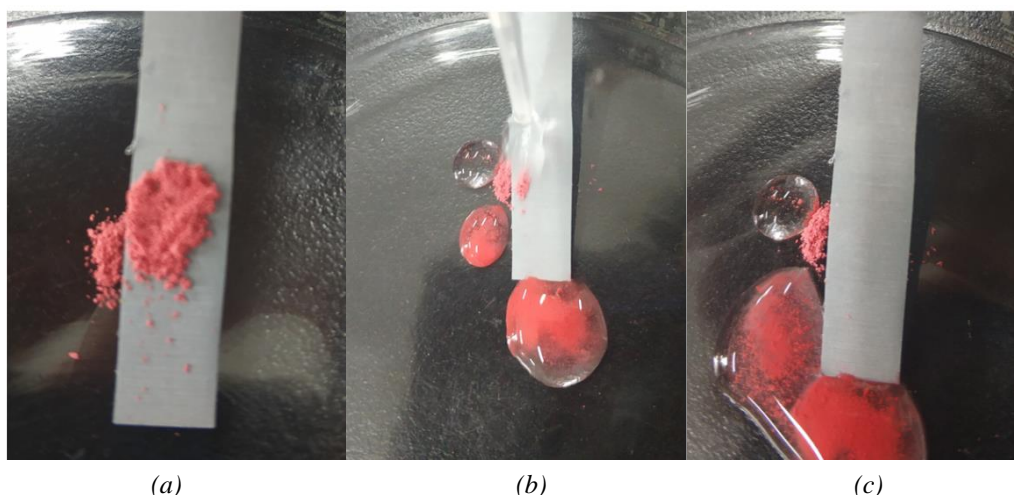


Fig. 4. Self-cleaning tests on the as-prepared superhydrophobic surface against chalk powder: (a) before, (b) during, and (c) after water droplets cleaning.

3.4. Oil-water separation

Because of the special wettability of hydrophobic and lipophilic, the biomimetic superhydrophobic network material can effectively separate oil and water selectively. Herein, a homemade oil-water separation device was used to test the separation performance of the sample (Fig.5a). The separation process is shown in Fig.5b-c. To separate edible oil-water mixture, diesel oil-water mixture, petroleum ether-water mixture, cyclohexane-water mixture and liquid paraffin-water mixture, respectively. The separation efficiencies are shown in Fig.5 d. It can be seen that all of the oil-water separation efficiencies are over 92%. At the same time, taking the separation of gasoline/water mixture as an example, the reusability of the as-prepared superhydrophobic samples was investigated. As shown in Fig.5e, after 10 cycles of separation tests, the separation efficiency did not decrease obviously. The above results show that the as-prepared superhydrophobic samples exhibited good oil-water separation property and reusability.

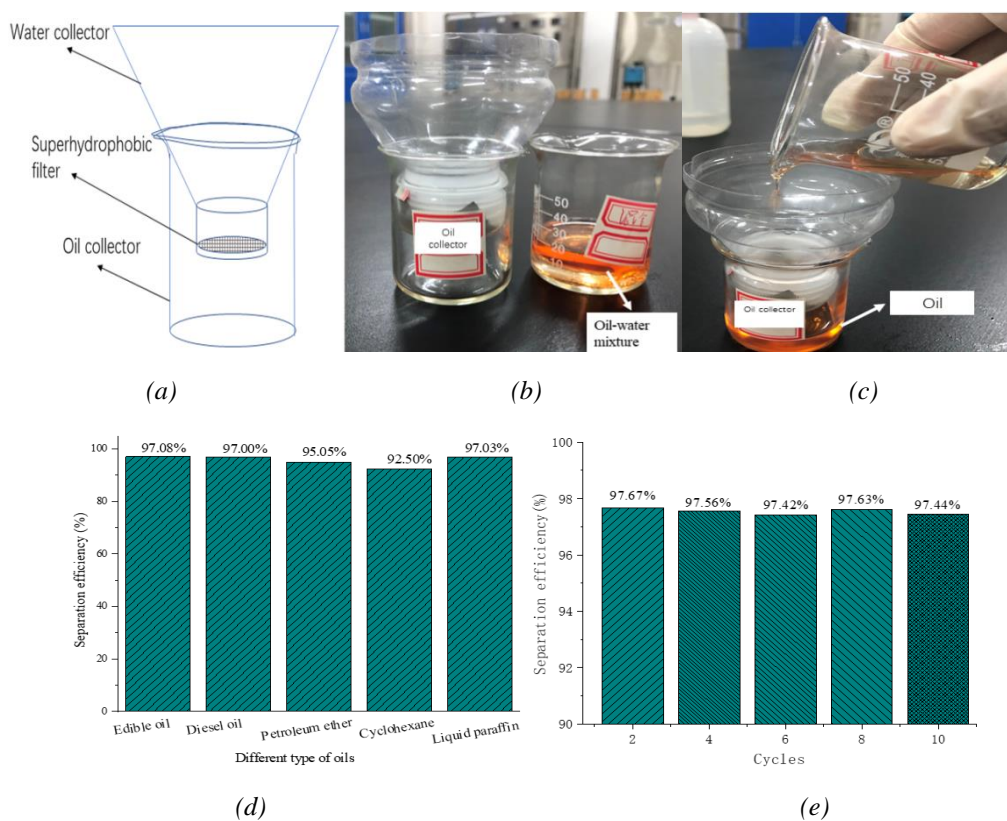


Fig. 5. (a) Schematic of oil/water separator. (b, c) Photographs of the oil/water mixture separation. (d) The separation efficiency of superhydrophobic stainless steel mesh for different kinds of oil/water mixtures. (e) The separation efficiency evaluation of the superhydrophobic stainless steel mesh in the isolation of gasoline from water over 10 cycles.

3.5. Wetting behavior of the as-prepared samples

Fig.6 shows the wettability of the blank mesh substrate and the as-prepared sample surface to water droplets. For the blank sample, the static contact angle to water is about 135° , which indicates that it is not superhydrophobic (Fig.6a, c). Due to the influence of gravity, the water droplet on the surface of superhydrophobic sample is slightly elliptical, and the contact angle is about 170.3° (Fig.6b, d), showing the excellent superhydrophobic property. When the water droplets contact the as-prepared sample surface, the surface can be regarded as the composite interface between the surface of micro/nano protrusion structure modified by stearic acid and air. According to the calculation formula for describing the contact angle of liquid-solid-gas three-phase composite interface proposed by Cassie et al. [31]:

$$\cos \theta_r = f_1 \cos \theta - f_2 \quad (2)$$

where f_1 and f_2 are the area ratio of liquid contacting solid surface and air respectively, $f_1 + f_2 = 1$, θ is the contact angle of liquid on smooth surface, and θ_r is the contact angle of liquid on rough composite surface. According to that equation, the ratio of air on the surface of superhydrophobic sample is 95.12%. It can be seen that the petal-like rough structure on the surface of the stainless steel mesh can store a large amount of air, and when water droplets contact the surface, the

solid-liquid-gas three-phase composite interface is conducive to reduce the contact area between the water droplets and the surface. At the same time, with the modification of stearic acid, a low surface energy material, the synergistic effect of the two gives the stainless steel mesh good superhydrophobic performance.

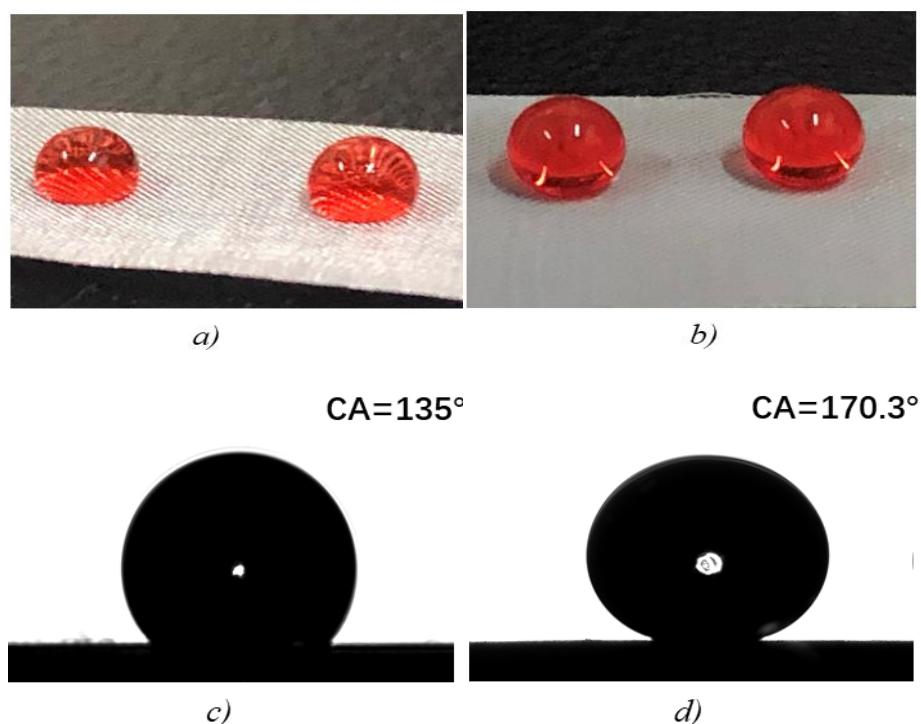


Fig. 6. Optical images of water droplets on the (a) bare stainless steel mesh substrate and (b) superhydrophobic stainless steel meshes. Profiles of water droplets on the (c) bare stainless steel mesh substrate (WCA = 135°) and (d) superhydrophobic stainless steel mesh (WCA = 170.3°).

Current density is one of the most important control conditions in electrodeposition process. Under the current density of $4.3 \text{ A} \cdot \text{dm}^{-2}$, $4.6 \text{ A} \cdot \text{dm}^{-2}$, $4.8 \text{ A} \cdot \text{dm}^{-2}$, $5.2 \text{ A} \cdot \text{dm}^{-2}$, $5.4 \text{ A} \cdot \text{dm}^{-2}$, $5.7 \text{ A} \cdot \text{dm}^{-2}$, and $6.0 \text{ A} \cdot \text{dm}^{-2}$, electroplating was carried out for 5 minutes respectively. The effect of current density on the wettability of the samples is shown in Fig.7. It can be seen that when the current density is $4.3 \text{ A} \cdot \text{dm}^{-2}$, the contact angle is 147.6° , which has not reached superhydrophobic. Further increasing the current density, the contact angle first increases and then decreases. When the current density was increased to $5.4 \text{ A} \cdot \text{dm}^{-2}$, the contact angle reached the maximum. The reason for the decrease of contact angle may be that with the further increase of current density, the surface petal-like structure will gradually grow into clusters, and the non-uniformity of surface roughness will increase, which will subsequently affect the role of the air in the gap to support the surface water droplets, resulting in the decline of overall hydrophobic performance.

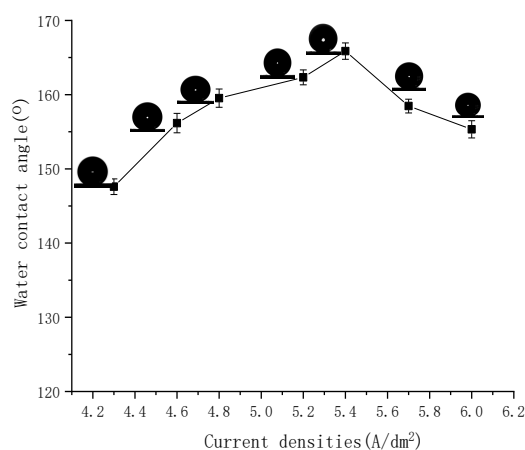


Fig. 7. Effect of current density on the wettability of the superhydrophobic stainless steel mesh.

To further investigate the effect of plating time on the wettability of the samples, the current density was fixed for $5.4 \text{ A} \cdot \text{dm}^{-2}$ and the samples were electroplated for 3 min, 5 min, 8 min, and 10 min, respectively. The effect of plating time on the wettability of the samples is shown in Fig.8. It can be seen that the electrodeposition time would directly affect the superhydrophobic properties of the samples. If the electrodeposition time is too long, it would lead to the thickness of the zinc coating, which would not only affect its superhydrophobicity, but also block the mesh of the matrix and affect its permeability. If the time is too short, the required microstructures can not be obtained, which would affect the superhydrophobic properties. When the electrodeposition time is 8 minutes, the contact angle is 170.3° . At this time, the contact angle is the largest and the thickness of the coating is uniform.

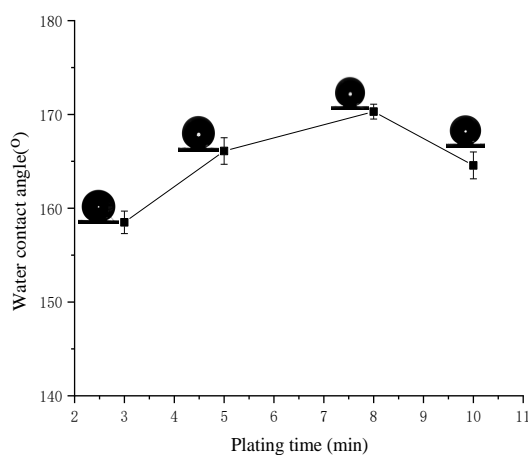


Fig. 8. Effect of plating time on the wettability of the superhydrophobic stainless steel mesh.

4. Conclusions

The robust superhydrophobic coating on stainless steel mesh substrate was prepared by electrodeposition combined with stearic acid modification. The effects of processing parameters on the wettability were studied. The current density and electrodeposition time seriously affect the

quality of samples, and then affect its superhydrophobic properties. The as-prepared superhydrophobic surfaces showed excellent water repellency, self-cleaning and mechanical durability. Remarkably, the prepared superhydrophobic surface still had superhydrophobic property after rubbing 230 cm distance on 600 grid sandpaper under 200 g loading. In addition, the as-prepared superhydrophobic filter also showed high oil-water separation efficiency and excellent reusability. This low-cost, environmentally friendly and simple preparation process can be used to develop large-scale, durable superhydrophobic coatings, and it is possible to achieve real industrial applications in many fields.

Acknowledgements

We gratefully acknowledge the National Natural Science Foundation of China (21171143) and the Key Research Fund Project of Xuchang University (2019ZD002).

References

- [1] J. R. Dong, J. S. Zeng, B. Wang, Z. Cheng, J. Xu, W. H. Gao, K. F. Chen, *ACS Applied Materials & Interfaces* (13), 15910(2021). <https://doi.org/10.1021/acsami.1c02394>
- [2] E. Nyankson, D. Rodene, R. B. Gupta, *Water Air & Soil Pollution*227(1), 29(2016). <https://doi.org/10.1007/s11270-015-2727-5>
- [3] M. A. Cohen, *Encyclopedia of Energy, Natural Resource, and Environmental Economics* 3(3), 121(2013) <https://doi.org/10.1016/B978-0-12-375067-9.00094-2>
- [4] M. Zhu, Y. C. Liu, M. Y. Chen, Z. H. Xu, L. L. Li, R. Liu, W. He, Y. Zhou, Y. Bai, *Langmuir* (37), 8776(2021). <https://doi.org/10.1021/acs.langmuir.1c01125>
- [5] R. Lakshmanan, C. Okoli, M. Boutonnet, S. Järås, G. K. Rajarao, *Bioresource Technology* (129), 612(2013). <https://doi.org/10.1016/j.biortech.2012.12.138>
- [6] G. Darracq, J. Baron, M. Joyeux, *Journal of Water Process Engineering* (3), 123(2014). <https://doi.org/10.1016/j.jwpe.2014.06.002>
- [7] Y. C. Liu, W. W. Tu, M. Y. Chen, L. L. Ma, B. Yang, Q. L. Liang, Y. Y. Chen, *Chemical Engineering Journal* (336), 263(2017). <https://doi.org/10.1016/j.cej.2017.12.043>
- [8] H. Wang, H. Chen, Y. Zeng, G. R. Chen, M. B. Cui, *Digest Journal of Nanomaterials and Biostructures* 16(2), 515 (2021).
- [9] G. G. Shi, M. M. Wu, Q. Zhong, P. Mu, J. Li, *Langmuir* 37 (25), 7843(2021) <https://doi.org/10.1021/acs.langmuir.1c01216>
- [10] X. Li, H. J. Yao, X. Lu, Z. Xin, *Industrial & Engineering Chemistry Research*60 (23), 8516(2021). <https://doi.org/10.1021/acs.iecr.1c00685>
- [11] F. Wang, S. Lei, C. Q. Li, J. F. Ou, *Industrial & Engineering Chemistry Research* 53(17), 7141(2014). <https://doi.org/10.1021/ie402584a>
- [12] T. Chen, Z.Y. Liu, K. Zhang, B. L. Su, Z. H. Hu, H. R. Wan, Y. Chen, X. K. Fu, Z. J. Gao, *ACS Applied Materials & Interfaces* 13 (42), 50539(2021). <https://doi.org/10.1021/acsami.1c14544>
- [13] X. H. Yan, X. Xiao, C. Au, S. Mathur, L. J. Huang, Y. X. Wang, Z. J. Zhang, Z. J. Zhu, M. J.

- Kipper, J. G. Tang, J. Chen, *Journal of Materials Chemistry A* 38(9), 21659(2021).
<https://doi.org/10.1039/D1TA05873H>
- [14] P. Phanthong, P. Reubroycharoen, S. Kongparakul, C. Samart, Z. D. Wang, X. G. Hao, A. Abudula, G. Q. Guan, *Carbohydrate Polymers* 190(1), 184(2018).
<https://doi.org/10.1016/j.carbpol.2018.02.066>
- [15] J. C. Gu, P. Xiao, Y. J. Huang, J. W. Zhang, *Journal of Materials Chemistry A* 3(8), 4124(2015). <https://doi.org/10.1039/C4TA07173E>
- [16] W. W. Zheng, J. Y. Huang, S. H. Li, M. Z. Ge, L. Teng, Z. Chen, Y. K. Lai, *ACS Applied Materials & Interfaces* (13), 67(2021). <https://doi.org/10.1021/acsami.0c18794>
- [17] L. Qiu, Y. H. Sun, Z. G. Guo, *Journal of Materials Chemistry A* (8), 16831(2020).
<https://doi.org/10.1039/D0TA02997A>
- [18] Y. C. Sang, A. B. Albadarin, A. H. Al-Muhtaseb, C. Mangwandi, J. N. McCracken, S. E. J. Bell, G. M. Walker, *Applied Surface Science* 335, 107(2015).
<https://doi.org/10.1016/j.apsusc.2015.02.034>
- [19] H. Y. Zhu, L. Gao, X. Q. Yu, C. H. Liang, *Appl Surf Sci* 407, 145(2017).
<https://doi.org/10.1016/j.apsusc.2017.02.184>
- [20] L. Feng, Z. Y. Zhang, Z. H. Mai, Y. M. Ma, B. Q. Liu, L. Jiang, D. B. Zhu, *Angewandte Chemie International Edition* 43(15), 2012(2004). <https://doi.org/10.1002/anie.200353381>
- [21] D. H. Wu, D. K. Li, X. Y. Gao, Z. G. Guo, *New Journal of Chemistry* 42(21), 17625(2018).
<https://doi.org/10.1039/C8NJ03980A>
- [22] L. Tie, J. Li, M. M. Liu, Z. G. Guo, Y. M. Liang, W. M. Liu, *ACS Applied Nano Materials* 1 (9), 4894(2018). <https://doi.org/10.1021/acsanm.8b01074>
- [23] J. Jeevahan, M. Chandrasekaran, G. Britto Joseph, R. B. Durairaj, G. Mageshwaran, *Journal of Coating Technology Research* (15), 231(2018). <https://doi.org/10.1007/s11998-017-0011-x>
- [24] E. Vazirinasab, R. Jafari, G. Momen, *Surface and Coating Technology* (341), 40(2018).
<https://doi.org/10.1016/j.surfcoat.2017.11.053>
- [25] Z. Chen, C. Zhu, M. L. Cai, X. Y. Yi, J. H. Li, *Applied Surface Science* (508), 145291(2020).
<https://doi.org/10.1016/j.apsusc.2020.145291>
- [26] S. Y. Wang, C. Hou, M. X. Wu, X. C. Li, *Colloids and Surfaces A Physicochemical and Engineering Aspects* 614(8), 126185(2021). <https://doi.org/10.1016/j.colsurfa.2021.126185>
- [27] H. Y. Wang, Y. X. Zhu, Z. Y. Hu, X. G. Zhang, S. Q. Wu, R. Wang, Y. J. Zhu, *Chemical Engineering Journal* 303(1), 37(2016). <https://doi.org/10.1016/j.cej.2016.05.133>
- [28] T. C. Chen, S. R. Ge, H. T. Liu, Q. H. Sun, W. Zhu, W. Yan, J. W. Qi, *Applied Surface Science* 356(30), 81(2015). <https://doi.org/10.1016/j.apsusc.2015.08.045>
- [29] Z. D. Wang, C. M. Xiao, Z. J. Wu, Y. T. Wang, X. Du, W. Kong, D. H. Pan, G. Q. Guan, X. G. Hao, *Journal of Materials Chemistry A* (5), 5895(2017). <https://doi.org/10.1039/C6TA10248D>
- [30] H. Shen, F. P. Wang, Y. W. Ding, J. Yang, *Acta Metallurgica Sinica(English Letters)* 26(6), 641(2013). <https://doi.org/10.1007/s40195-013-0226-5>
- [31] A. B. D. Cassie, S. Baxter, *Transactions of the Faraday Society* 40(1), 546(1944).
<https://doi.org/10.1039/tf9444000546>